Mycorrhiza (1996) 6:431–440

ORIGINAL PAPER

Michelle Schelkle · Margot Ursic · Melissa Farquhar
R. Larry Peterson

The use of laser scanning confocal microscopy to characterize mycorrhizas of *Pinus strobus* L. and to localize associated bacteria

Accepted: 17 July 1996

Abstract Laser scanning confocal microscopy (LSCM), light microscopy (LM) and epifluorescence microscopy (FM) were used to observe the extramatrical hyphae, mantle patterns and associated bacteria on mycorrhizal tips of *Pinus strobus* L. seedlings grown in pot cultures. *Laccaria* sp. and *Tuber* sp. formed ectomycorrhizas with *Pinus strobus,* while *Phialophora finlandia* Wang & Wilcox and E-strain (sensu Danielson 1982) formed ectendomycorrhizas. Distinct mantle patterns and cystidia were observed with greater resolution using LSCM, and intracellular hyphae were visualized in three dimensions. Trypan blue penetrated fresh whole mounts to 20 μm and was an excellent stain for visualizing fungal hyphae and bacteria with LSCM. Fluorescein isothiocyanate and acridine orange were used in conjunction with LSCM and FM to localize bacteria on ectomycorrhizal tips. With LSCM, bacteria were visible in the surface mucigel, and optical sectioning through the root tip showed that bacteria were also present within the mantle. LSCM is a non-intrusive and fast method for visualizing mycorrhizal structures and their associated bacteria on fresh, whole root tips.

Key words Ectomycorrhizas · *Pinus strobus* · Bacteria · Confocal microscopy

Introduction

Laser scanning confocal microscopy (LSCM), a relatively new light microscopic imaging technique, has been used effectively to demonstrate structural characteristics of some plant-fungal associations in situ (Czymmek et al. 1994; Kobayashi et al. 1994). This is possible because the LSCM can collect "optical slices" through thick sections without physically sectioning, and then reconstruct these slices to form a three-dimensional (3-D) image (Cox 1993). LSCM thus provides a means of observing the spatial organization of fungal and bacterial associations in intact plant tissues without harsh clearing techniques or physical sectioning of the plant material.

The previous identification of ectomycorrhizas (ECM) and localization of associated bacteria had relied upon light microscopy (LM), epifluorescence microscopy (FM), scanning electron microscopy (SEM) and transmission electron microscopy (TEM). The potential of LSCM to facilitate observations of mycorrhizal fungal and bacterial colonization in situ had not been explored.

Ectomycorrhizas can be identified, or at least categorized into morphological types (morpho-types), based on their mantle patterns and the presence or absence of other characteristic structures such as cystidia, clamp connections and hyphal ornamentation (Agerer 1991; Haug and Oberwinkler 1987; Haug and Pritsch 1992; Ingleby et al. 1990). Typically, light microscopy (LM) is used to visualize the mantle patterns but it is often difficult to obtain clear pictures of each distinct mantle layer and its associated structures. When using fresh, whole mounts, particularly of tips with darkly pigmented mantles, mantle patterns are obscured because of inadequate quantities of light passing through the tissue. Routine solutions to this problem include peeling off the mantle or taking paradermal sections of the root tip, but both these techniques involve a high degree of root tip manipulation and manual dexterity. Cystidia (terminal hyphae which emanate from basidiomycete or ascomycete structures) are usually easier to visualize with LM than the mantle itself, but often cross several planes of focus and are difficult to photograph clearly in their entirety when using light microscopy.

Intracellular hyphae, the diagnostic structures for ectendotrophism, are typically observed with LM using thin hand sections of fresh material or sections of fixed and resin embedded ectendomycorrhizal root tips.

M. Schelkle · M. Ursic · M. Farquhar · R. L. Peterson (✉)
Department of Botany, University of Guelph, Guelph, Ontario N1G 2W1, Canada
fax: +1-519-767-1991; e-mail: lpeterso@uoguelph.ca

While resolution is not a problem, these images fail to convey the three-dimensional nature of the structures involved. In addition, artefacts may be present in resin-embedded material because of the processing involved during fixation and embedding.

Associated with ECM, rhizosphere bacteria have been shown to promote mycorrhizal development (Duponnois and Garbaye 1990; Garbaye and Bowen 1989; Garbaye and Duponnois 1992). Visualization of these bacteria on and within the ECM mantle normally involves careful fixing, embedding and sectioning of the root tissue for TEM (Filippi et al. 1995; Foster and Marks 1967; Malajczuk 1979) or dehydrating and drying for SEM. Both techniques involve intensive preparation and produce only very limited information about the bacterial cells in relation to the rest of the mycorrhizal tissue.

In view of these difficulties, LSCM was explored as a method of overcoming the limitations of more conventional microscopy techniques. The specific objective of this present study was to examine the advantages and disadvantages of LSCM over other conventional methods for visualizing diagnostic features of ECM root tips and their associated bacteria on *Pinus strobus* L. seedlings.

Materials and methods

Seedling inoculation

Two ECM fungi (*Laccaria* sp. and *Tuber* sp.) and two ectendomycorrhizal fungi [E-strain sensu Danielson (1982) and *Phialophora finlandia* Wang & Wilcox] were used as inocula. *Laccaria* sp. was isolated from sporocarps found in the white pine (*Pinus strobus* L.) seedbeds at St. Williams, Ontario, Ministry of Natural Resources (OMNR) nursery (42°42′N, 80°27′W) in September 1994. The other fungi were isolated from mycorrhizal root tips of 2- and 3-year-old *Pinus strobus* seedlings from the same location following the method described by Kronick (1995).

Fungal isolates were cultured on 1.2% Modified Melin Norkrans medium (MMN) (Marx 1969) at room temperature (approx. 20 °C) in the dark for 4–8 weeks. Plugs (7-mm diameter) were removed from the margins of the colonies and aseptically scattered at 3 cm and 1 cm below the surface of the autoclaved potting medium (10% sand, 10% surface, 80% perlite) in surface-sterilized 6 in. pots. Twenty plugs were scattered at each depth for a total of 40 plugs per pot.

Concurrent with fungal inoculation of the potting medium, seeds of *Pinus strobus* were placed in the pots. Seeds obtained from St. Williams OMNR nursery (seedlots #72-80 and #72-70) were surface sterilized in 5% hypochlorite solution (Javex) for 12 min, rinsed in deionized water (3 × 200 ml), rinsed in sterile water (2 × 200 ml), dried and stratified overnight at 4 °C. Eight seeds were aseptically placed in each pot above the top layer of fungal plugs and covered with potting mix. Sterile liquid MMN solution (40 ml) and sterile distilled water (100 ml) were added to each pot. The pots were sealed in sterile Sunpac™ bags (Sigma) with 0.2-μm filters for gas exchange for the course of the study. Bagged pots were kept in a growth chamber with an 8-h photoperiod (110–150 $\mu E\ m^{-2}\ s^{-1}$, fluorescent and incandescent lamps) at 80% humidity and 20 °C for the first 8 weeks, then at 24 °C for the remaining period. Each pot received 100 ml of sterile distilled water at 4-week intervals administered in the flow hood.

Microscopy

The seedlings were harvested and examined after 12–14 weeks of growth. Ectomycorrhizal root tips of *Pinus strobus* were examined with a Zeiss dissecting microscope for the gross morphological characteristics of the different types. Mycorrhizal roots, characterized by slightly blunted tips, few or no root hairs and hyphae appressed against the root surface, were excised from the main root and prepared immediately for microscopy. At least 10 tips from each fungal treatment were viewed for each staining regimen.

For LM, fresh whole tips were placed on a slide and mounted directly into either water, lactophenol blue (1% aniline blue in lactophenol) (Gerlach 1969), or 0.05% trypan blue (1 part 85% lactic acid, 2 parts glycerol and 1 part distilled water) (Peacock 1966). In addition to being observed fresh, mycorrhizal tips of E-strain and *Phialophora finlandia* were fixed and embedded to prepare them for microtome sectioning. Tips were fixed in 3% glutaraldehyde in sodium phosphate buffer (pH 6–8) for at least 4 h, dehydrated in a graded ethanol series and gradually embedded with LR White resin as described by Brundrett et al. (1994). Polymerized tips were thick sectioned with glass knives on an OmU3 C Reichert microtome. Sections were stained with methylene blue-azur B (1% methylene blue, 1% azur B, 1% sodium borate in distilled water). Observations were made with a Leitz Orthoplan bright field microscope and photographs were taken with Kodak T-Max 400 or Ilford Pan-F film.

For LSCM, fresh whole root tips were excised from the main root and stained with a variety of fluorochromes to evaluate the suitability of these dyes for imaging of ECM and bacteria. Tips dyed with fluorescein isothiocyanate (FITC) staining solution (0.25 ml of 0.5 M carbonate buffer pH 9.5, 1.1 ml of 0.01 M phosphate buffer pH 7.2, 1.1 ml of 0.85% NaCl and 1.0 mg FITC) were stained for 5 min, rinsed 3 times with 0.5 M carbonate buffer (pH 9.5) and mounted in this buffer (Sherr et al. 1993). Acridine orange (AO) (0.1% in phosphate buffer pH 6.3) was allowed to stain for 20–30 min, after which the tips were rinsed twice in phosphate buffer and mounted in the same buffer (Kasten 1981). Tips were stained in fluorescent Schiff's reagent (0.5% acriflavine hydrochloride, 1% potassium metabisulphite, 10% 1 N HCl) for 30 min, rinsed 3 times in distilled water and mounted in water (Culling 1974). Root tips stained with 0.05% trypan blue were simply mounted in the freshly made stain.

Observations were made using a BIO-RAD MRC 600 laser scanning confocal microscope equipped with a Nikon fluorescent microscope and a Krypton-Argon mixed gas laser. Samples stained with FITC and AO were viewed using photomultiplier (PMT) detector 2 (< 560 nm emission wavelength) while those stained with fluorescent Schiff's reagent and trypan blue used the PMT detector 1 (> 560 nm emission wavelength). Optical slices were taken at various depths in the tissues using a 60× oil immersion lens. Series of optical slices taken at 1-μm intervals were reconstructed to visualize 3-D features on the exterior of the mantles. Images were shot as black and white negatives using a Polaroid slide shooter and Ilford Pan-X film from which prints were made.

Root tips viewed with conventional FM were stained using the same techniques as for LSCM. Only *Tuber* sp. tips were used. Slides were viewed under blue light using a Leitz epifluorescence microscope equipped with an excitation filter BE 12/TK and barrier filter 510/K515. Photographs were taken with Kodak T-Max 400.

Terminology

There is no standard set of terms for describing the morphology of ECM tips. This paper adopts the terms used by Ingleby et al. (1990) to describe mantle patterns, mantle layers, and structures emanating from the mantle. The five basic mantle patterns are 'felt prosenchyma' (hyphal cells are distinctly elongated and disorganized), 'net prosenchyma' (hyphal cells are still distinct and

septate but wider and loosely organized), 'net synenchyma' (cells are still hyphal in appearance but closely appressed and labyrinthine in form), 'irregular synenchyma' (hyphal cells are pseudoparenchymatous, closely appressed and ovoid to jigsaw-puzzle shaped) and 'regular synenchyma' (hyphal cells are pseudoparenchymatous, closely appressed and more or less isodiametric). Mantle layers are referred to as D1 for the outermost, D2 for the second distinct layer, and so on.

Results

There was considerable variation in staining results depending on the microscopic technique employed and the type of material observed (Table 1).

Visualization of ecto- and ectendomycorrhizal structures

Of the fluorochromes tested, freshly-made trypan blue was the most effective stain for LSCM imaging of ECM mantles and structures associated with the mantle. FITC, AO and fluorescent Schiff's reagent resulted in faint and inconsistent fluorescence of the fungal tissue. Conventional FM of ECM tips was problematic because the copious background fluorescence emanating from layers above and below the plane of focus hindered image resolution (Table 1).

Structures emanating from the ECM mantles, such as cystidia on the *Tuber* sp. tips and external hyphae with clamp connections on the *Laccaria* sp. tips, were easier to observe and photograph with LSCM than with conventional LM. The LSCM's ability to clearly reconstruct several trypan blue-stained *Tuber* sp. cystidia and the adjoining mantle hyphae by accumulating series of optical slices resulted in a clearer, more informative image than LM, which allowed only one cystidium to be focussed on and left unresolvable those cystidia beyond the plane of focus (compare Fig. 1 to Fig. 5). In addition, staining *Tuber* sp. ECM tips with either lactophenol blue (Fig. 5) or trypan blue (not shown) for LM obscured the connection between the cystidia and the mantle because more stain bound to the mantle than to the emanating hyphae.

Although viewing distinct ECM mantle layers was possible with both LM and LSCM, the latter technique proved much more effective for distinguishing and photographing the different layers and also permitted calculation of the distance between successive layers. Figs. 2–4 show LSCM optical slices of *Tuber* sp. mycorrhizas taken at the same x-y location on the mantle but at different depths. In comparison, Figs. 6–8 show comparable layers viewed with LM. The transition from a net prosenchyma organization on the D1 mantle layer to an irregular synenchyma in the deeper layers (D2 and D3) of *Tuber* sp. was apparent with both types of microscopy. However, with LSCM, bacteria were visible in the interhyphal spaces in the D1 and D2 layers (Figs. 2, 3) but notably absent in the D3 layer (Fig. 4). The fluorescence of the fungal cell walls provided evidence of stain penetration into the D3 layer, indicating that the absence of bacteria was not an artifact. In addition, each distinct mantle layer was determined to be 5 μm deeper than the next using LSCM. This was accomplished by using the calibrated focus motor which moves the microscope stage in known increments. Unfortunately, even with LSCM, none of the stains employed were able to penetrate adequately more than 20–25 μm into the ECM root tips, reducing resolution of the D3 mantle layer and beyond.

Trypan blue was an excellent stain to image the mantle using LSCM, but poor for visualizing mantle patterns with LM because it stained surface hyphae very darkly and in an irregular manner while staining underlying hyphae very faintly. Unstained ECM tips could be used for LM, but better contrast was obtained with lactophenol blue. Tips stained with lactophenol blue showed more distinct hyphal walls creating a clearer mantle pattern (Figs. 6, 7, 14, 15) than unstained tips viewed with LM (Figs. 8, 13).

Table 1 A summary of the stains used to visualize rhizosphere bacteria and ectomycorrhizal fungi with light, epifluorescence and laser scanning confocal microscopy (*FITC* fluorescein isothiocyanate)

Microscopy	Stain	Fungi		Bacteria	
		Resolution	Contrast	Resolution	Contrast
Light	No stain	Good	Poor	Poor	Poor
	Trypan blue	Poor	Poor	Poor	Poor
	Lactophenol blue	Good	Good	Poor	Poor
Epifluorescence	FITC	Poor	Good	Poor	Good
	Acridine orange	Poor	Good	Poor	Good
Laser scanning confocal	FITC[a]	Good	Excellent	Excellent	Excellent
	Acridine orange[a]	Poor	Poor	Good	Excellent
	Schiff's reagent[b]	Poor	Poor	Poor	Poor
	Trypan blue[b]	Excellent	Excellent	Excellent	Excellent

[a] <560 nm emission
[b] >560 nm emission

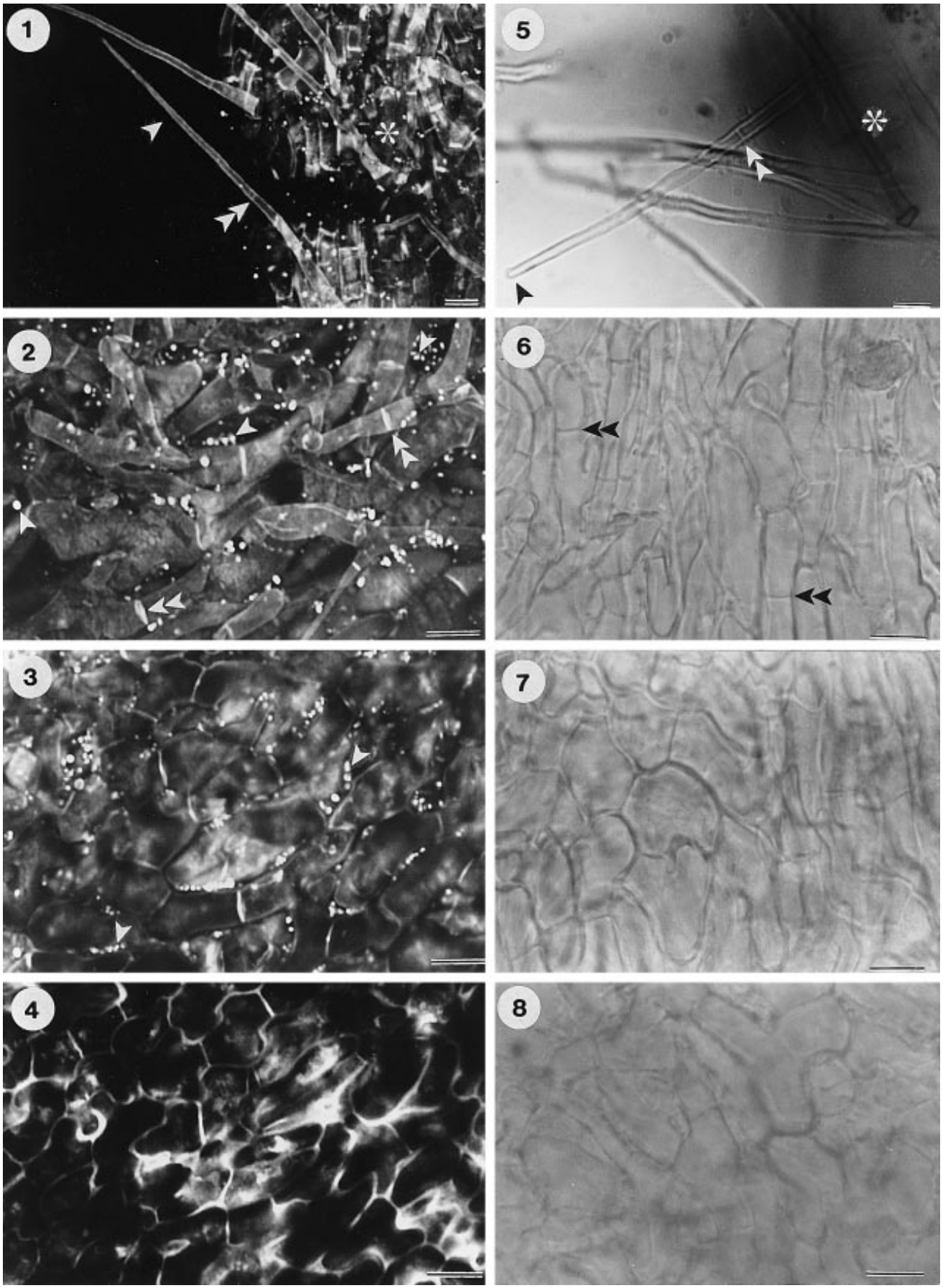
1
5
2
6
3
7
4
8

Observation of the ectendomycorrhizal mantles and intracellular hyphae was also improved with LSCM. Hyphal elements and septation could be seen with greater resolution than with LM (compare Figs. 9–11 to Figs. 13–15). Distinct mantle layers of E-strain tips were calculated with the LSCM to be 5 μm apart. Because E-strain and *Philaphora finlandia* mantles were quite thin, trypan blue was able to penetrate into the epidermal and outermost layer of cortical cells so that coiled intracellular hyphae could be seen in situ (Fig. 12). Without LSCM, observations such as these would have been virtually impossible to obtain with fresh whole mounts. Usually, intracellular hyphae of ectendomycorrhizas are examined using embedded sections (Fig. 16) (see also Scales and Peterson 1991). Sectioning of the resin-embedded root tissue destroys the three-dimensionality of these hyphal coils within the cortical cells and limits interpretation of the structure in its entirety. Unfortunately, LSCM imaging of intracellular colonization beyond the outermost layer of root cortical cells was prevented by poor stain infiltration into deeper layers of the tissue.

Figs. 1–4 Cystidia and mantle features of a fresh, whole ectomycorrhiza formed between *Tuber* sp. and *Pinus strobus* L., mounted in 0.05% trypan blue and viewed with laser scanning confocal microscopy (LSCM); *bars* 10 μm

Fig. 1 A Z-series reconstruction of a cystidium (*single arrowhead*) emanating from a *Tuber* sp. mante (*asterisk*). A basal septum (*double arrowhead*) and acute tip are evident

Figs. 2–4 A series of optical slices of a *Tuber* sp. mantle taken at the same x-y location but at different depths (*single arrowheads* bacteria, *double arrowheads* septa)

Fig. 2 Outermost (D1) mantle layer in a net prosenchyma pattern with numerous bacteria in the interhyphal spaces

Fig. 3 Second (D2) layer showing a net – irregular synenchyma pattern with bacteria still evident in the interhyphal spaces

Fig. 4 Innermost (D3) mantle layer showing the irregular synenchyma pattern diagnostic of *Tuber* sp. Bacteria are notably absent at this depth in the mantle

Figs. 5–7 Cystidia and mantle features of fresh, whole ectomycorrhizas formed between *Tuber* sp. and *Pinus strobus* mounted in lactophenol blue and viewed with light microscopy (LM); *bars* 10 μm

Fig. 5 A cystidium in the forefront with an acute tip (*single arrowhead*) and basal septum (*double arrowhead*) emanating from the mantle (*asterisk*). Background cystidia are out of focus

Fig. 6 The D1-D2 layer of a *Tuber* sp. mycorrhiza with a net synenchyma organization. Septa are evident (*double arrowheads*)

Fig. 7 The D2-D3 layer seen in the same location as in Fig. 6 but at a deeper focal plane, showing an irregular synenchyma pattern diagnostic of *Tuber* sp.

Fig. 8 A view of the D2 layer of a *Tuber* sp. – *Pinus strobus* ectomycorrhiza, unstained and viewed with LM; *bar* 10 μm

Localization of bacteria

Bacteria were present in all pots examined, presumably because soil sterilization was not effective in killing all bacterial propagules. Of the fluorochromes tested, trypan blue, FITC and AO were all very effective in staining the bacteria associated with ECM mantles on *Pinus strobus.* With conventional FM, AO proved to be a better stain than FITC or trypan blue for visualizing bacteria (Table 1). With the latter two stains, only a few bacterial cells in the D1 layers of the mantle were visible at any one time, and the hyphae were unresolvable due to the intensity of background fluorescence (Fig. 17). On tips stained with AO, the bacteria were easily discernable against the mantle because the hyphae did not pick up the stain, limiting information regarding the fungus (Fig. 18).

Images obtained with LSCM were much clearer than those obtained with FM. Samples stained with FITC (Figs. 19, 21, 22) and trypan blue (Figs. 2, 3) provided more information concerning the spatial arrangement of the bacteria and the hyphae than root tips stained with AO (Fig. 20). With AO, the hyphae stained sporadically, making it difficult to determine the layers of the mantle with which the bacteria were associated; bacteria were only clearly visible in the surface mucigel. An optical section of the D2 layer in the mantle of a *Tuber* sp. ECM stained with FITC clearly showed bacteria located in pockets between the closely-packed hyphae (Fig. 21). Regular hyphal septation is also evident. At a higher magnification of the same location, the resolution of the image began to decline, although rod-shaped bacterial cells could still be seen in the interhyphal spaces (Fig. 22).

Discussion

Identification of ECM is an important prerequisite for any attempt to examine the richness or abundance of these fungi. Keys using mantle patterns in combination with other diagnostic morphological features (Agerer 1991; Haug and Pritsch 1992; Ingleby et al. 1990) illustrate that it is possible, albeit often difficult, to obtain identifications without reference to fungal cultures or molecular methods. Although identification based on morphology may only allow placement of an ECM tip into a "morpho-type" or a genus, it is an effective method of estimating species richness when numerous samples are being examined.

LSCM allows morpho-types to be viewed and photographed as easily and with greater clarity than with conventional LM. Furthermore, LSCM allows thicknesses of distinct mantle layers to be measured and intracellular hyphae to be visualized in three dimensions, neither of which are possible with whole, fresh mounts viewed with LM. One drawback of LSCM is that it requires bright fluorescence of the tissues or structures of interest. Trypan blue worked well as a fluorescent stain


9

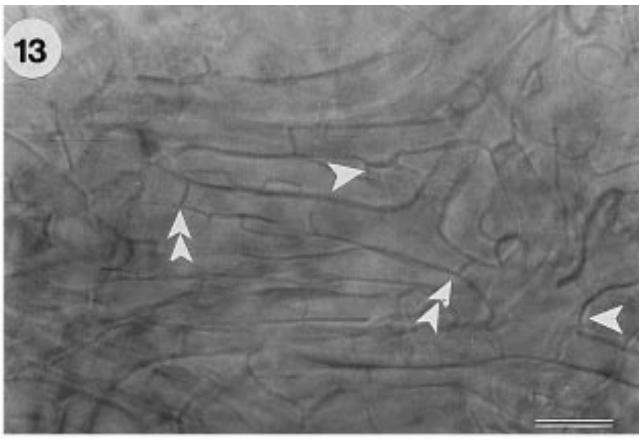
13

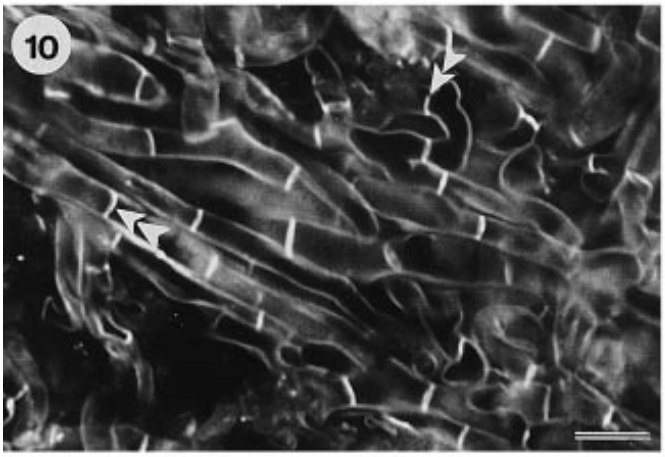
10

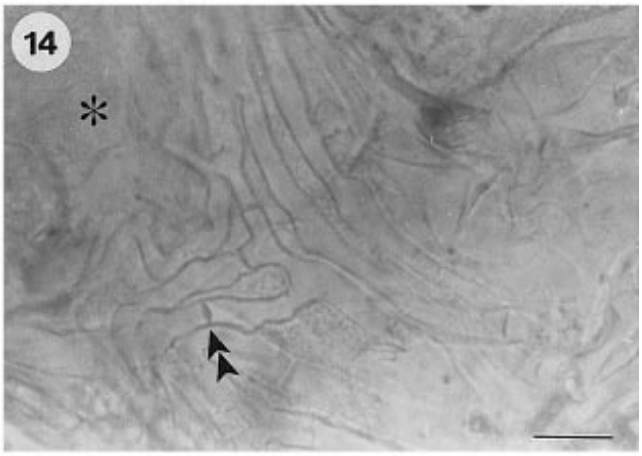
14

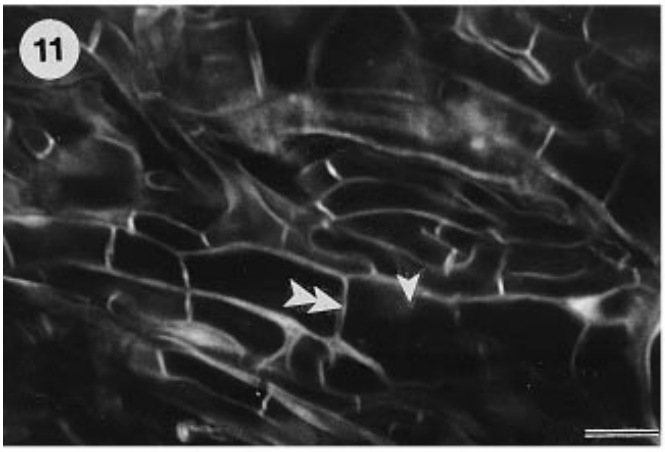
11

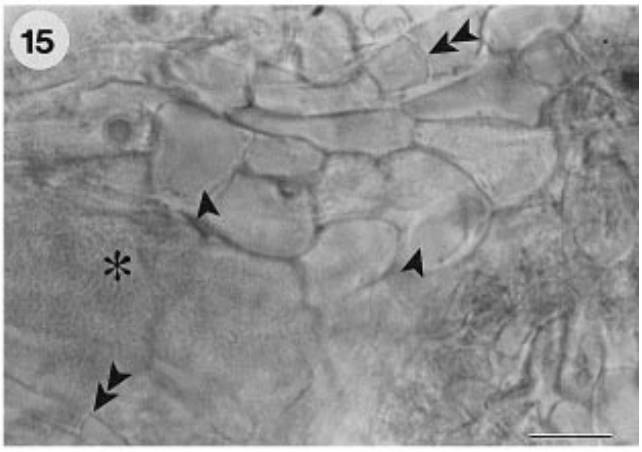
15

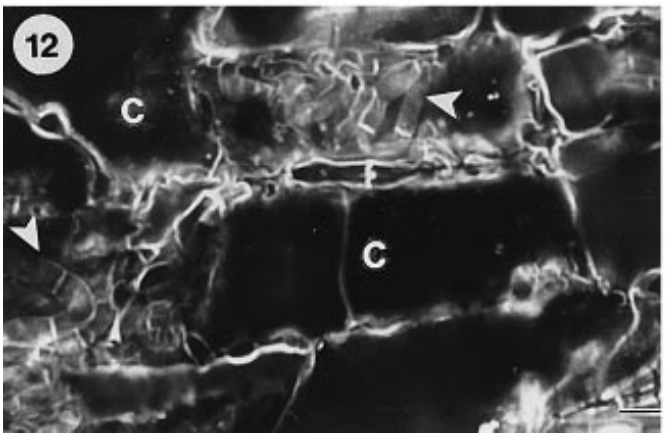
12
C
C


16
M
M
E
C

with the four fungal species used in this study, but it is not known whether the binding properties of the stain are similar for all fungal species.

Trypan blue fluorescence of ECM root tips is unsuitable for use with the conventional FM because the fluorescence from other focal planes is too intense to allow detailed resolution. LSCM, in comparison, can eliminate background fluorescence to give a sharp, detailed image. Notably, the fluorescence activity of trypan blue was found to be ephemeral and dependent upon the use of freshly made stain. For this reason, trypan blue stain is inappropriate when LSCM observation can not be undertaken immediately following staining.

Figs. 9–12 Mantle layers and intracellular hyphae of a mycorrhiza formed between E-strain and *Pinus strobus* L. Fresh, whole root tips were mounted in 0.05% trypan blue and viewed with LSCM (*double arrowheads* hyphal septa); *bars* 10 μm

Fig. 9 D1 mantle layer showing a loose net prosenchyma organization. A few clusters of bacteria (*single arrowheads*) are evident

Figs. 10–12 Successive layers of an E-strain – *Pinus strobus* L. mycorrhiza visualized at different depths in the same location. Bacteria are notably absent

Fig. 10 D1 mantle layer showing a loosely organized net prosenchyma

Fig. 11 D2 mantle layer showing a net prosenchyma – net synenchyma organization with some wide hyphal cells (*single arrowhead*)

Fig. 12 Coiled intracellular hyphae (*single arrowheads*) are evident in the root cortical cells (*C*) 6 μm deeper than the D2 mantle layer. A few bacteria are seen in one of the cells with intracellular hyphal penetration

Figs. 13–16 Mantle layers and intracellular hyphae of E-strain – *Pinus strobus* mycorrhizas viewed with conventional LM; *bars* 10 μm

Fig. 13 The D1 mantle layer as seen on a whole, fresh, unstained root tip. Hyphal septa (*double arrowheads*) and H-type anastamoses (*single arrowheads*) are evident in this loose net prosenchyma organization

Figs. 14–15 Successive layers of an E-strain mantle visualized at different depths in the same location. This fresh, whole mount was stained with lactophenol blue. Portions of the mantle at slightly different planes of focus are noticeably blurred (*asterisks*) (*double arrowheads* hyphal septa)

Fig. 14 D1 mantle layer showing a loose net prosenchyma pattern with hyphae of irregular widths

Fig. 15 D2 mantle layer showing a net – irregular synenchyma pattern with some wide hyphal cells (*single arrowheads*)

Fig. 16 Enlarged portion of a longitudinal section of an E-strain – *Pinus strobus* mycorrhiza embedded with LR White, sectioned, and stained with methylene blue-azur B. A thin, loosely packed mantle (*M*) and discontinuous Hartig net (*single arrowheads*) around the epidermal (*E*) and cortical (*C*) cells can be seen. Intracellular hyphae (*double arrowheads*) are also evident. The other intracellular structures in the endodermal cells (*asterisks*) are starch grains

Regardless of the duration of staining, the depth to which the stain penetrated was always limited to about 20 μm. In this study, all the mycorrhizas were quite young and had relatively thin mantles, so it was possible to visualize all mantle layers and even the Hartig net or intracellular hyphae in the epidermal and cortical cells. If mantles are older and thicker, observing beyond the D2 layer may be difficult due to both a lack of stain infiltration and an inability of the laser beam to penetrate the dense, phenolic-rich tissue layers. In this respect, however, LSCM is no worse than LM.

Following ECM colonization, changes in root exudates result in a greater number of microbes in the rhizosphere and a change in the species types found (Linderman 1988; Malajczuk 1979; Oswald and Ferchau 1968). The bacteria seen associated with the *Pinus strobus* ECM in this study were rod-shaped or ovoid. Rods are characteristic of the most common soil bacteria, including *Pseudomonas, Bacillus, Xanthomonas, Flavobacterium* and *Clostridium* spp. (Atlas and Bartha 1993). The ovoid shape is characteristic of other common soil bacteria such as *Corynebacterium, Arthrobacter* and *Acinetobacter* spp. (Atlas and Bartha 1993; Stevenson 1989).

There is accumulating evidence that bacteria play an important role in the formation and proliferation of ECM tips. In vitro and in vivo synthesis studies have shown that certain species of rhizosphere bacteria such as *Pseudomonas* sp. and *Bacillus* sp. are able to promote mycorrhizal development (Garbaye and Bowen 1989; Duponnois and Garbaye 1990; Garbaye and Duponnois 1992). Their localization will contribute to our understanding of their roles.

Visualization of bacteria on mycorrhizal tissue is normally accomplished using TEM, which requires that the root tips be fixed, dehydrated, embedded, sectioned and stained with heavy metals (Buscot 1994; Danell et al. 1993; Filippi et al. 1995; Foster and Marks 1967; Malajczuk 1979). Similarly, SEM requires fixation, dehydration and coating the sample with gold/palladium. With LSCM, fresh whole mounts need only be stained before use. Not only is this much faster and easier than the time-consuming tissue preparation required for SEM or TEM, but it prevents the mucigel layer around the root tip from being disturbed. One disadvantage of LSCM for visualization of bacteria is that the magnification is limited to the confines of a regular light microscope and consequently the ultrastructure of bacterial cells is not discernable. TEM remains the best method if ultrastructural information is required.

Bacteria were observed primarily on the surface of the mantle and in the interhyphal spaces, which is consistent with the results of other TEM studies. Foster and Marks (1967) found bacterial cells deep within the mantle and the interhyphal spaces of *Pinus radiata* D. Don ECM. Similarly, Oswald and Ferchau (1968) observed aggregations of bacteria solely in the interhyphal mantle spaces of ECM tips of several conifer species. This contrasts with the results of Malajczuk (1979),

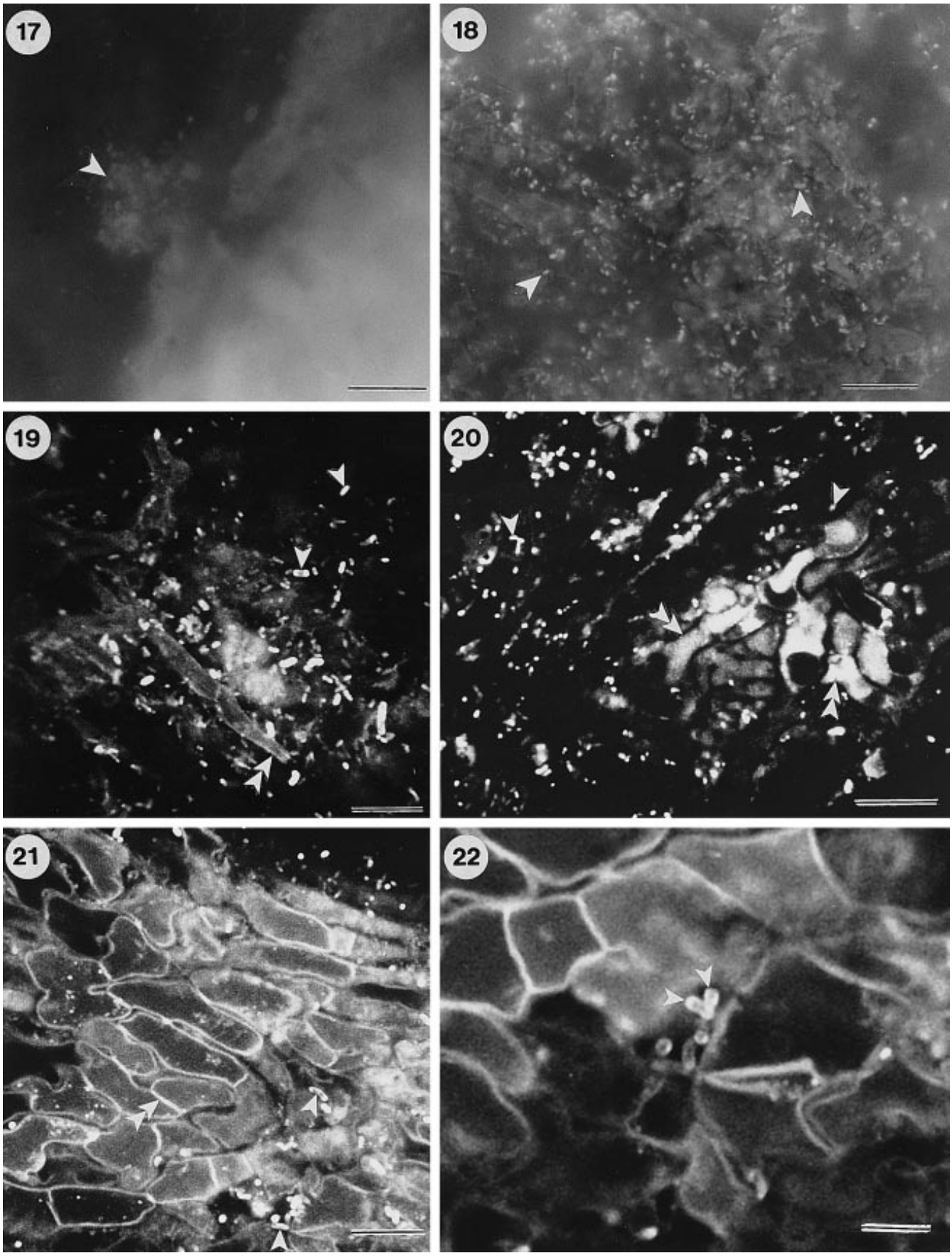
17
18
19
20
21
22

who found bacteria both between and within the mantle cells of *Pisolithus tinctorius* and *Eucalyptus* spp. Danell et al. (1993) suggested that *Cantharellus cibarius,* an ECM fungus associated with *Pinus* spp., may interweave microbes between its hyphal cells during the development of fruitbodies. A similar mechanism may account for the distribution of bacteria throughout the mantle in *Tuber* sp.-*Pinus strobus* ECM in this study. It is also possible that bacteria enter physiologically weaker or senescing cells as suggested by Filippi et al. (1995). In their study, *Azospirillum*-like bacteria were found between and within fungal hyphae of healthy arbutoid mycorrhizas, and within epidermal cells containing fungal hyphae in senescing mycorrizas. In our investigation, the hyphae appeared to be healthy and showed no visible signs of degeneration and no intracellular bacteria were visible. ECM formed between *Phialophora finlandia* or E-strain and *Pinus strobus* had fewer bacteria associated with the mantle; this may be due either to the limited development of the mantle or to the nature of the mucilage secreted by these fungi.

The use of FITC in conjunction with LSCM is excellent for visualizing bacteria on mycorrhizal tissue. The bacteria were clearly visible against the hyphae, and the ability to optically section through the material gave more accurate information about the location of associated bacteria than was possible with the other microscopy techniques. Furthermore, the ease with which the samples could be prepared was unrivalled, and in situ observation of extramatrical hyphae and bacteria in field-harvested material could perhaps be facilitated. Despite limited magnification, LSCM is a significant improvement over conventional FM. Although it is not practical to undertake all morpho-typing using this technique, LSCM is suggested as a technique for accurately documenting the various mantle layers and diagnostic features of ECM to aid morpho-typing.

Acknowledgements We would like to thank the Natural Sciences and Engineering Research Council of Canada for funding this project, and Mike Rose at St. Williams OMNR nusery for donation of the *Pinus strobus* seeds.

Figs. 17–22 Visualization of rhizosphere bacteria on ectomycorrhizas formed by *Tuber* spp. on *Pinus strobus* L. seedlings

Fig. 17 Fresh whole mount of a mycorrhizal tip stained with *fluorescein* isothiocyanate (FITC) and viewed with conventional FM using blue excitation filters. A bacterial colony (*single arrowhead*) is barely distinguishable; *bar* 10 μm

Fig. 18 Fresh whole mount of a mycorrhizal tip stained with acridine orange (AO) and viewed with conventional FM using blue excitation filters. Bacteria (*single arrowheads*) are clearly visible; *bar* 10 μm

Fig. 19 D1 of *Tuber* sp. mantle stained with FITC and viewed with LSCM. Numerous bacteria (*single arrowheads*) can be observed embedded in the mucigel with hyphae (*double arrowhead*) visible below this layer; *bar* 10 μm

Fig. 20 Whole mount of a *Tuber* sp. ectomycorrhiza stained with AO and viewed with LSCM. The outer mucigel layer is visible and contains many bacteria (*single arrowheads*). The hyphae have stained sporadically (*double arrowheads*) and only on the surface of the mantle; *bar* 10 μm

Fig. 21 The D2 layer of the same *Tuber* sp. mantle as viewed in Fig. 20 (stained with FITC and viewed with LSCM). Bacteria have aggregated in the interhyphal spaces (*single arrowheads*) and hyphal septations can be seen (*double arrowheads*) in the net synenchyma mantle pattern; *bar* 10 μm

Fig. 22 A higher magnification of Fig. 21. Rod-shaped bacteria can be seen between the hyphae (*single arrowheads*). The hyphae appear healthy and undamaged, suggesting that the bacteria are not having a negative effect; *bar* 2 μm

References

Agerer R (1991) Color atlas of ectomycorrhiza. Einhorn, Schwäbisch Gmünd

Atlas RM, Bartha R (1993) Microbial ecology. Benjamin/Cummings, Redwood City, pp 276–281

Brundrett M, Melville L, Peterson RL (1994) Practical methods in mycorrhiza research. Mycologue, Sidney, BC

Buscot F (1994) Ectomycorrhizal types and endobacteria associated with ectomycorrhizas of *Morchella elata* (Fr.) Boudier with *Picea abies* Karst. Mycorrhiza 4:223–232

Cox G (1993) Trends in confocal microscopy. In: Horne RW, Cockayne DJH, Harris JR (eds) Micron. Pergamon, London, pp 237–247

Culling CF (1974) Modern microscopy: elementary theory and practice. Butterworth, London

Czymmek KJ, Whallon JH, Klomparens KL (1994) Confocal microscopy in mycological research. Exp Mycol 18:275–293

Danell E, Alstrom S, Ternstrom A (1993) *Pseudomonas fluorescens* in association with the fruit bodies of the ectomycorrhizal mushroom *Cantharellus cibarius.* Mycol Res 97:1148–1152

Danielson RM (1982) Taxonomic affinities and criteria for identification of the common ectendomycorrhizal symbiont of pines. Can J Bot 60:7–18

Duponnois R, Garbaye J (1990) Some mechanisms involved in growth stimulation of ectomycorrhizal fungi by bacteria. Can J Bot 68:2148–2152

Filippi C, Bagnoli G, Giovannetti M (1995) Bacteria associated to arbutoid mycorrhizae in *Arbutus unedo* L. Symbiosis 18:57–68

Foster RC, Marks GC (1967) Observations on the mycorrhizas of forest trees. Austr J Biol Sci 20:915–926

Garbaye J, Bowen GD (1989) Stimulation of ectomycorrhizal infection of *Pinus radiata* by some microorganisms associated with the mantle of ectomycorrhizas. New Phytol 112:383–388

Garbaye J, Duponnois R (1992) Specificity and function of mycorrhization helper bacteria (MHB) associated with the *Pseudotsuga menziessi – Laccaria laccata* symbiosis. Symbiosis 14:335–344

Gerlach D (1969) Botanisch Mikrotechnik. Thieme. Stuttgart

Haug I, Oberwinkler F (1987) Some distinctive types of spruce mycorrhizae. Trees 1:172–188

Haug I, Pritsch K (1992) Ectomycorrhizal types of spruce [*Picea abies* (L.) Karst.] in the black forest. A microscopical atlas. Kernforschungszentrum, Karlsruhe

Ingleby K, Mason PA, Last FT, Fleming LV (1990) Identification of ectomycorrhizas. ITE Research Publication No. 5. HMSO, London

Kasten F (1981) Methods for fluorescence microsopy. In: Clark G (ed) Staining procedure, 4th edn. Waverley, Baltimore

Kobayashi I, Kobayashi Y, Hardham A (1994) Dynamic reorganization of microtubules and microfilaments in flax cells during the resistance response to flax rust infection. Planta 195:237–247

Kronick M (1995) Identification and relative abundances of mycorrhizal fungi on *Pinus strobus* L. nursery seedlings affected by root rot. MSc thesis, University of Guelph

Linderman RG (1988) Mycorrhizal interactions with the rhizosphere microflora: the mycorrhizosphere effect. Phytopathology 78:366–371

Malajczuk N (1979) The microflora of unsuberized roots of *Eucalyptus calophylla* R. Br. and *Eucalyptus marginata* Donn ex Sm. seedlings grown in soils suppressive and conductive to *Phytophthora cinnamomi* Rands. II. Mycorrhizal roots and associated microflora. Aust J Bot 27:235–254

Marx DH (1969) The influence of ectotrophic mycorrhizal fungi on the resistance to pathogenic infections. I. Antagonism of mycorrhizal fungi to pathogenic fungi and soil bacteria. Phytopathology 59:153–163

Oswald ET, Ferchau HA (1968) Bacterial associations of coniferous mycorrhizae. Plant Soil 28:187–192

Peacock HA (1966) Elementary microtechnique, 3rd edn. Arnold, London

Scales PF, Peterson RL (1991) Structure and development of *Pinus banksiana / Wilcoxina* ectendomycorrhizae. Can J Bot 69:2135–2148

Sherr EB, Caron DA, Sherr BF (1993) Staining of heterotrophic protists for visualization via epifluorescence microscopy. In: Kemp PF, Sherr BF, Sherr EB, Cole JJ (eds) Handbook of methods in aquatic microbial ecology. Lewis, London, pp 213–240

Stevenson RMW (1989) A field guide to systematic bacteriology. Department of Microbiology, University of Guelph, Guelph, pp 112–142